INTERNATIONAL JOURNAL FOR NUMERICAL METHODS IN FLUIDS, VOL. 9, 305–323 (1989)

COMPUTATION OF 3D VORTEX FLOWS PAST A FLAT PLATE AT INCIDENCE THROUGH A VARIATIONAL APPROACH OF THE FULL STEADY EULER EQUATIONS

CHARLES-HENRI BRUNEAU AND JACQUES LAMINIE
Laboratoire d'Analyse Numérique, Université Paris-Sud, 91405 Orsay Cédex, France

AND

JEAN-JACQUES CHATTOT
Aérospatiale, 78133 Les Mureaux, France

SUMMARY

A variational method for solving directly the full steady Euler equations is presented. This method is based on both Newton's linearization and a least squares formulation. The validity of the Euler model and boundary conditions to capture the vortex sheet is discussed. A finite element approximation of the groups of conservative variables is described and results are given for 3D subsonic flows as well as supersonic flows past a flat plate at high angle of attack.

KEY WORDS Steady Euler equations Variational method 3D vortex flows Finite element approximation Newton linearization Least-squares formulation Subsonic and supersonic flows

INTRODUCTION

In the last few years intensive studies have been done by many researchers on numerical computation of vortical flows around wings; in particular, around swept and delta wings using steady or unsteady Euler or Navier–Stokes models (see for instance References 1–3 and references therein). Vortex-dominated flows are of primary interest in aeronautics and space technologies; indeed vortices developing above the wing induce low pressure on the upper surface and consequently yield an additional lift. Numerous questions still remain; among them we can point out:

1. Where and when does separation occur, in particular on smooth surfaces?
2. Is the Euler model able to capture separation on a sharp or on a smooth leading edge without the help of artificial viscosity?
3. How do vortex sheets develop in relation to the Mach number at infinity and the angle of attack?

0271–2091/89/030305–19$09.50

Received 2 February 1988
Revised 13 May 1988

At the First International Conference on Industrial and Applied Mathematics (Paris 1987) several numerical solutions of vortex-dominated flows around wings were presented; in particular A. Rizzi showed solutions about a swept wing with a rounded leading edge calculated from Euler and Navier–Stokes equations. He noticed that separation occurs in both cases but is located more upstream with the Navier–Stokes model, and that the vortex sheets are quite different in shape and growth. We believe that, even with the same mathematical model, artificial viscosity and numerical dissipation yield quite different vortex sheets from one method to another, especially when a smooth leading edge and complex geometry are concerned.

In this paper we choose to study a very simple geometry, a rectangular flat plate of zero thickness. This choice eliminates the difficulty of separation on smooth surfaces and allows us to use the Euler model because the separation does not result from viscous effects. Indeed separation occurs at the leading edge and the vortex structure rolls up at the tip of the plate, grows until the trailing edge and is convected beyond. Our aim is to show that such inviscid separation can be obtained from Euler equations which allow rotational effects, without the help of artificial viscosity or the Kutta condition, and to give some partial answers to the main questions above.

In the next section we present the variational method we use to study the full steady Euler equations; we then discuss the appropriate boundary conditions, the finite element approximation, the numerical method to solve the linear system and the implementation. The last section is devoted to numerical results for several Mach numbers at infinity, angles of attack and meshes.

DESCRIPTION OF THE METHOD

In previous works in 2D and 3D[4, 5] we used Bernoulli's theorem for steady flows to reduce the equation of conservation of energy to its algebraic form and to write consequently a fixed point algorithm on the density. Here we write the whole system as conservative partial differential equations in a 3D domain Ω as follows:

$$\begin{aligned}
\frac{\partial \rho u}{\partial x}+\frac{\partial \rho v}{\partial y}+\frac{\partial \rho w}{\partial z}&=0,\\
\frac{\partial \rho u^2}{\partial x}+\frac{\partial \rho uv}{\partial y}+\frac{\partial \rho uw}{\partial z}+\frac{\partial(\gamma-1)\rho e}{\partial x}&=0,\\
\frac{\partial \rho uv}{\partial x}+\frac{\partial \rho v^2}{\partial y}+\frac{\partial \rho vw}{\partial z}+\frac{\partial(\gamma-1)\rho e}{\partial y}&=0,\\
\frac{\partial \rho uw}{\partial x}+\frac{\partial \rho vw}{\partial y}+\frac{\partial \rho w^2}{\partial z}+\frac{\partial(\gamma-1)\rho e}{\partial z}&=0,\\
\frac{\partial(\gamma\rho e+\frac{1}{2}\rho q^2)u}{\partial x}+\frac{\partial(\gamma\rho e+\frac{1}{2}\rho q^2)v}{\partial y}+\frac{\partial(\gamma\rho e+\frac{1}{2}\rho q^2)w}{\partial z}&=0,
\end{aligned} \tag{1}$$

where we recognize the equation of conservation of mass, the three equations of conservation of momentum and the equation of conservation of energy for the density ρ, the three components of the velocity $\mathbf{q}=(u, v, w)$ and the specific internal energy as unknowns. We denote by q the modulus of $\mathbf{q}$ and by γ the ratio of specific heats. One notices that the hypothesis of a perfect gas with constant specific heats is made and that the pressure and the total enthalpy are replaced by

$(\gamma-1)\rho e$ and $\gamma e+\frac{1}{2}q^2$ respectively. Here these equations are associated with Dirichlet boundary conditions on the plate and at the far-field boundaries of the domain; we impose a tangency condition (as is usual for the Euler model) on both sides of the plate ($\mathbf{q}\cdot\mathbf{n}=0$, where $\mathbf{n}$ is the unit normal pointing out from the plate), a symmetry condition on the plate $y=0$ (see Figure 1) and some other conditions at the far-field boundaries which are discussed in the next section.

For the sake of simplicity we present the method in dimension two; the first idea is to linearize the first-order hyperbolic non-linear operator L appearing in (1) by the Newton method. Indeed the strong non-linearity of the conservative terms with respect to the unknowns in (1) and our wish to keep the groups of conservative variables to enforce the conservation properties do not allow us to write directly a variational formulation. Let us denote the unknowns by $\mathbf{U}^{\mathrm{T}}=(\rho, u, v, e)$; then we solve $L(\mathbf{U})=0$ by means of the algorithm

$$\begin{cases}\mathbf{U}_0 \text{ given},\\ \mathbf{U}_{m+1}=\mathbf{U}_m-\tilde{\mathbf{U}}, \quad m=0,\ldots,p,\end{cases}$$

where $\tilde{\mathbf{U}}^{\mathrm{T}}=(\tilde\rho, \tilde u, \tilde v, \tilde e)$ is the solution of the linear system

$$\begin{aligned}
&\frac{\partial\tilde\rho u_m}{\partial x}+\frac{\partial\tilde\rho v_m}{\partial y}+\frac{\partial\rho_m\tilde u}{\partial x}+\frac{\partial\rho_m\tilde v}{\partial y}=\frac{\partial\rho_m u_m}{\partial x}+\frac{\partial\rho_m v_m}{\partial y},\\
&\frac{\partial\tilde\rho u_m^2}{\partial x}+\frac{\partial\tilde\rho u_m v_m}{\partial y}+\frac{\partial(\gamma-1)\tilde\rho e_m}{\partial x}+\frac{\partial 2\rho_m u_m\tilde u}{\partial x}+\frac{\partial\rho_m\tilde u v_m}{\partial y}+\frac{\partial\rho_m u_m\tilde v}{\partial y}+\frac{\partial(\gamma-1)\rho_m\tilde e}{\partial x}\\
&\qquad=\frac{\partial\rho_m u_m^2}{\partial x}+\frac{\partial\rho_m u_m v_m}{\partial y}+\frac{\partial(\gamma-1)\rho_m e_m}{\partial x},\\
&\frac{\partial\tilde\rho u_m v_m}{\partial x}+\frac{\partial\tilde\rho v_m^2}{\partial y}+\frac{\partial(\gamma-1)\tilde\rho e_m}{\partial y}+\frac{\partial\rho_m\tilde u v_m}{\partial x}+\frac{\partial\rho_m u_m\tilde v}{\partial x}+\frac{\partial 2\rho_m v_m\tilde v}{\partial y}+\frac{\partial(\gamma-1)\rho_m\tilde e}{\partial y}\\
&\qquad=\frac{\partial\rho_m u_m v_m}{\partial x}+\frac{\partial\rho_m v_m^2}{\partial y}+\frac{\partial(\gamma-1)\rho_m e_m}{\partial y},\\
&\frac{\partial\tilde\rho(\gamma e_m+\frac{1}{2}q_m^2)u_m}{\partial x}+\frac{\partial\tilde\rho(\gamma e_m+\frac{1}{2}q_m^2)v_m}{\partial y}+\frac{\partial\gamma\rho_m e_m\tilde u}{\partial x}+\frac{\partial\frac{3}{2}\rho_m u_m^2\tilde u+\frac{1}{2}\rho_m v_m^2\tilde u}{\partial x}\\
&\quad+\frac{\partial\rho_m u_m\tilde u v_m}{\partial y}+\frac{\partial\gamma\rho_m e_m\tilde v}{\partial y}+\frac{\partial\frac{3}{2}\rho_m v_m^2\tilde v+\frac{1}{2}\rho_m u_m^2\tilde v}{\partial y}+\frac{\partial\rho_m v_m\tilde v u_m}{\partial x}+\frac{\partial\gamma\rho_m\tilde e u_m}{\partial x}+\frac{\partial\gamma\rho_m\tilde e v_m}{\partial y}\\
&\qquad=\frac{\partial(\gamma\rho_m e_m+\frac{1}{2}\rho_m q_m^2)u_m}{\partial x}+\frac{\partial(\gamma\rho_m e_m+\frac{1}{2}\rho_m q_m^2)v_m}{\partial y}
\end{aligned}\tag{2}$$

associated with some boundary conditions. Thus at each step of the Newton linearization $\tilde{\mathbf{U}}$ is the solution of a linear problem

$$\begin{cases}\mathbf{A}\tilde{\mathbf{U}}=\mathbf{F},\\ \tilde{\mathbf{U}}\in\mathscr{D}(\mathbf{A}),\end{cases}\tag{3}$$

where $\mathscr{D}(\mathbf{A})$ is a space we define more precisely later with Dirichlet boundary conditions for $\tilde{\mathbf{U}}$ which are homogeneous because $\mathbf{U}_0$ is given satisfying the Dirichlet boundary conditions of the

initial problem. In the following we drop the subscript m; thus the operator $\mathbf{A}$ reads

$$\mathbf{A}=\begin{bmatrix} \frac{\partial u\cdot}{\partial x}+\frac{\partial v\cdot}{\partial y} & \frac{\partial \rho\cdot}{\partial x} & \frac{\partial \rho\cdot}{\partial y} & 0 \\ \frac{\partial[u^2+(\gamma-1)e]\cdot}{\partial x}+\frac{\partial uv\cdot}{\partial y} & \frac{\partial 2\rho u\cdot}{\partial x}+\frac{\partial \rho v\cdot}{\partial y} & \frac{\partial \rho u\cdot}{\partial y} & \frac{\partial(\gamma-1)\rho\cdot}{\partial x} \\ \frac{\partial uv\cdot}{\partial x}+\frac{\partial[v^2+(\gamma-1)e]\cdot}{\partial y} & \frac{\partial \rho v\cdot}{\partial x} & \frac{\partial \rho u\cdot}{\partial x}+\frac{\partial 2\rho v\cdot}{\partial y} & \frac{\partial(\gamma-1)\rho\cdot}{\partial y} \\ \frac{\partial(\gamma eu+\frac{1}{2}q^2u)\cdot}{\partial x} & \frac{\partial \gamma\rho e\cdot}{\partial x}+\frac{\partial(\frac{3}{2}\rho u^2+\frac{1}{2}\rho v^2)\cdot}{\partial x} & \frac{\partial \gamma\rho e\cdot}{\partial y}+\frac{\partial(\frac{3}{2}\rho v^2+\frac{1}{2}\rho u^2)\cdot}{\partial y} & \frac{\partial \gamma\rho u\cdot}{\partial x} \\ +\frac{\partial(\gamma ev+\frac{1}{2}q^2v)\cdot}{\partial y} & +\frac{\partial \rho uv\cdot}{\partial y} & +\frac{\partial \rho vu\cdot}{\partial x} & +\frac{\partial \gamma\rho v\cdot}{\partial y} \end{bmatrix}$$

and the vector $\mathbf{F}$ is the left-hand side of (1) written in dimension two. Thus Newton linearization leads us to solve p times a linear problem with a first-order hyperbolic operator still which has the same characteristic curves as the initial one. Indeed, let φ be a function constant on the characteristic curves and φ_x, φ_y be the components of grad φ; then the characteristic polynomial is given by the following determinant simplified by linear combinations of rows and columns (since in system (3), $\mathbf{U}$ is assumed to be regular enough to write $\mathbf{A}$ in its non-conservative form):

$$\begin{bmatrix} u\varphi_x+v\varphi_y & \rho\varphi_x & \rho\varphi_y & 0 \\ 0 & \rho(u\varphi_x+v\varphi_y) & 0 & (\gamma-1)\rho\varphi_x \\ 0 & 0 & \rho(u\varphi_x+v\varphi_y) & (\gamma-1)\rho\varphi_y \\ -\gamma e(u\varphi_x+v\varphi_y) & 0 & 0 & \rho(u\varphi_x+v\varphi_y) \end{bmatrix}$$

$$=\rho^3(u\varphi_x+v\varphi_y)^2[(u\varphi_x+v\varphi_y)^2-\gamma e(\gamma-1)(\varphi_x^2+\varphi_y^2)].$$

As $\mathrm{d}\varphi=0$ on the characteristic curves, by setting $\tau=\mathrm{d}y/\mathrm{d}x=-\varphi_x/\varphi_y$ we get

$$\det=\rho^3\varphi_y^4(-\tau u+v)^2[(-\tau u+v)^2-\gamma e(\gamma-1)(\tau^2+1)]$$

and thus the streamlines are zeros of multiplicity two. Moreover, we have two additional real roots when the Mach number is greater than or equal to one. Finally, we find that the linear operator has the well known characteristic curves of the Euler system and thus the same hyperbolic behaviour. This remark leads us to the second idea, which is to solve the linear system (3) by means of a least squares method. Thus we minimize over the space $\mathscr{D}(\mathbf{A})$ the functional

$$J(\tilde{\mathbf{U}})=\frac{1}{2}\int_\Omega\left(\frac{\partial\tilde\rho u}{\partial x}+\frac{\partial\tilde\rho v}{\partial y}+\frac{\partial\rho\tilde u}{\partial x}+\frac{\partial\rho\tilde v}{\partial y}-\frac{\partial\rho u}{\partial x}-\frac{\partial\rho v}{\partial y}\right)^2\mathrm{d}x\mathrm{d}y$$

$$+\frac{1}{2}\int_\Omega\left(\frac{\partial\tilde\rho u^2}{\partial x}+\frac{\partial\tilde\rho uv}{\partial y}+\frac{\partial(\gamma-1)\tilde\rho e}{\partial x}+\frac{\partial 2\rho u\tilde u}{\partial x}+\frac{\partial\rho\tilde uv}{\partial y}+\frac{\partial\rho u\tilde v}{\partial y}+\frac{\partial(\gamma-1)\rho\tilde e}{\partial x}\right.$$

$$\left.-\frac{\partial\rho u^2}{\partial x}-\frac{\partial\rho uv}{\partial y}-\frac{\partial(\gamma-1)\rho e}{\partial x}\right)^2\mathrm{d}x\mathrm{d}y$$

$$+\frac{1}{2}\int_\Omega\left(\frac{\partial\tilde\rho uv}{\partial x}+\frac{\partial\tilde\rho v^2}{\partial y}+\frac{\partial(\gamma-1)\tilde\rho e}{\partial y}+\frac{\partial\rho\tilde uv}{\partial x}+\frac{\partial\rho u\tilde v}{\partial x}+\frac{\partial 2\rho v\tilde v}{\partial y}+\frac{\partial(\gamma-1)\rho\tilde e}{\partial y}\right.$$

$$-\frac{\partial \rho uv}{\partial x}-\frac{\partial \rho v^2}{\partial y}-\frac{\partial(\gamma-1)\rho e}{\partial y}\Bigg)^2 \mathrm{d}x\mathrm{d}y$$
$$+\frac{1}{2}\int_\Omega\Bigg(\frac{\partial \tilde{\rho}(\gamma e+\frac{1}{2}q^2)u}{\partial x}+\frac{\partial \tilde{\rho}(\gamma e+\frac{1}{2}q^2)v}{\partial y}+\frac{\partial \gamma \rho e\tilde{u}}{\partial x}+\frac{\partial \frac{3}{2}\rho u^2\tilde{u}+\frac{1}{2}\rho v^2\tilde{u}}{\partial x}$$
$$+\frac{\partial \rho u\tilde{u}v}{\partial y}+\frac{\partial \gamma \rho e\tilde{v}}{\partial y}+\frac{\partial \frac{3}{2}\rho v^2\tilde{v}+\frac{1}{2}\rho u^2\tilde{v}}{\partial y}+\frac{\partial \rho v\tilde{v}u}{\partial x}+\frac{\partial \gamma \rho \tilde{e}u}{\partial x}+\frac{\partial \gamma \rho \tilde{e}v}{\partial y}$$
$$-\frac{\partial(\gamma \rho e+\frac{1}{2}\rho q^2)u}{\partial x}-\frac{\partial(\gamma \rho e+\frac{1}{2}\rho q^2)v}{\partial y}\Bigg)^2 \mathrm{d}x\mathrm{d}y$$

and, computing the Gateau derivative G of J with respect to the unknowns, we get the variational formulation

$$\begin{cases}\text{find } \tilde{\mathbf{U}}\in\mathscr{D}(\mathbf{A}) \text{ such that}\\ \langle G(\tilde{\mathbf{U}}),\bar{\mathbf{U}}\rangle=0 \quad \forall \bar{\mathbf{U}}\in\mathscr{D}(\mathbf{A}),\end{cases} \tag{4}$$

where

$$\langle G(\tilde{\mathbf{U}}),\bar{\mathbf{U}}\rangle=\int_\Omega\Bigg(\frac{\partial \tilde{\rho}u}{\partial x}+\frac{\partial \tilde{\rho}v}{\partial y}+\frac{\partial \rho\tilde{u}}{\partial x}+\frac{\partial \rho\tilde{v}}{\partial y}-\frac{\partial \rho u}{\partial x}-\frac{\partial \rho v}{\partial y}\Bigg)\Bigg(\frac{\partial \bar{\rho}u}{\partial x}+\frac{\partial \bar{\rho}v}{\partial y}+\frac{\partial \rho\bar{u}}{\partial x}+\frac{\partial \rho\bar{v}}{\partial y}\Bigg)\mathrm{d}x\mathrm{d}y$$
$$+\int_\Omega\Bigg(\frac{\partial \tilde{\rho}u^2}{\partial x}+\frac{\partial \tilde{\rho}uv}{\partial y}+\frac{\partial(\gamma-1)\tilde{\rho}e}{\partial x}+\frac{\partial 2\rho u\tilde{u}}{\partial x}+\frac{\partial \rho\tilde{u}v}{\partial y}+\frac{\partial \rho u\tilde{v}}{\partial y}+\frac{\partial(\gamma-1)\rho\tilde{e}}{\partial x}$$
$$-\frac{\partial \rho u^2}{\partial x}-\frac{\partial \rho uv}{\partial y}-\frac{\partial(\gamma-1)\rho e}{\partial x}\Bigg)$$
$$\times\Bigg(\frac{\partial \bar{\rho}u^2}{\partial x}+\frac{\partial \bar{\rho}uv}{\partial y}+\frac{\partial(\gamma-1)\bar{\rho}e}{\partial x}+\frac{\partial 2\rho u\bar{u}}{\partial x}+\frac{\partial \rho\bar{u}v}{\partial y}+\frac{\partial \rho u\bar{v}}{\partial y}+\frac{\partial(\gamma-1)\rho\bar{e}}{\partial x}\Bigg)\mathrm{d}x\mathrm{d}y$$
$$+\int_\Omega\Bigg(\frac{\partial \tilde{\rho}uv}{\partial x}+\frac{\partial \tilde{\rho}v^2}{\partial y}+\frac{\partial(\gamma-1)\tilde{\rho}e}{\partial y}+\frac{\partial \rho\tilde{u}v}{\partial x}+\frac{\partial \rho u\tilde{v}}{\partial x}+\frac{\partial 2\rho v\tilde{v}}{\partial y}+\frac{\partial(\gamma-1)\rho\tilde{e}}{\partial y}$$
$$-\frac{\partial \rho uv}{\partial x}-\frac{\partial \rho v^2}{\partial y}-\frac{\partial(\gamma-1)\rho e}{\partial y}\Bigg)$$
$$\times\Bigg(\frac{\partial \bar{\rho}uv}{\partial x}+\frac{\partial \bar{\rho}v^2}{\partial y}+\frac{\partial(\gamma-1)\bar{\rho}e}{\partial y}+\frac{\partial \rho\bar{u}v}{\partial x}+\frac{\partial \rho u\bar{v}}{\partial x}+\frac{\partial 2\rho v\bar{v}}{\partial y}+\frac{\partial(\gamma-1)\rho\bar{e}}{\partial y}\Bigg)\mathrm{d}x\mathrm{d}y$$
$$+\int_\Omega\Bigg(\frac{\partial \tilde{\rho}(\gamma e+\frac{1}{2}q^2)u}{\partial x}+\frac{\partial \tilde{\rho}(\gamma e+\frac{1}{2}q^2)v}{\partial y}+\frac{\partial \gamma\rho e\tilde{u}}{\partial x}+\frac{\partial \frac{3}{2}\rho u^2\tilde{u}+\frac{1}{2}\rho v^2\tilde{u}}{\partial x}$$
$$+\frac{\partial \rho u\tilde{u}v}{\partial y}+\frac{\partial \gamma\rho e\tilde{v}}{\partial y}+\frac{\partial \frac{3}{2}\rho v^2\tilde{v}+\frac{1}{2}\rho u^2\tilde{v}}{\partial y}+\frac{\partial \rho v\tilde{v}u}{\partial x}+\frac{\partial \gamma\rho\tilde{e}u}{\partial x}+\frac{\partial \gamma\rho\tilde{e}v}{\partial y}$$
$$-\frac{\partial(\gamma\rho e+\frac{1}{2}\rho q^2)u}{\partial x}-\frac{\partial(\gamma\rho e+\frac{1}{2}\rho q^2)v}{\partial y}\Bigg)$$
$$\times\Bigg(\frac{\partial \bar{\rho}(\gamma e+\frac{1}{2}q^2)u}{\partial x}+\frac{\partial \bar{\rho}(\gamma e+\frac{1}{2}q^2)v}{\partial y}+\frac{\partial \gamma\rho e\bar{u}}{\partial x}+\frac{\partial \frac{3}{2}\rho u^2\bar{u}+\frac{1}{2}\rho v^2\bar{u}}{\partial x}$$
$$+\frac{\partial \rho u\bar{u}v}{\partial y}+\frac{\partial \gamma\rho e\bar{v}}{\partial y}+\frac{\partial \frac{3}{2}\rho v^2\bar{v}+\frac{1}{2}\rho u^2\bar{v}}{\partial y}+\frac{\partial \rho v\bar{v}u}{\partial x}+\frac{\partial \gamma\rho\bar{e}u}{\partial x}+\frac{\partial \gamma\rho\bar{e}v}{\partial y}\Bigg)\mathrm{d}x\mathrm{d}y.$$

All the above formulae are meaningful if we define the following spaces:

$$\mathscr{V} = \{\mathbf{U} \in (L^\infty(\Omega)^4,\ \mathbf{U} > \mathbf{0} \text{ such that } L(\mathbf{U}) \in (L^2(\Omega))^4\},$$

$$\tilde{\mathscr{V}} = \{\tilde{\mathbf{U}} \in (L^2(\Omega))^4 \text{ such that } \mathbf{A}\tilde{\mathbf{U}} \in (L^2(\Omega))^4\},$$

$$\mathscr{D}(\mathbf{A}) = \{\tilde{\mathbf{U}} \in \tilde{\mathscr{V}} \text{ satisfying some homogeneous Dirichlet boundary conditions}\}.$$

We notice that the initial variables (components or groups of components of $\mathbf{U}$) appearing in $\mathbf{A}\tilde{\mathbf{U}}$ can be considered as positive weights in $\tilde{\mathscr{V}}$; we shall make precise the boundary conditions of $\mathscr{D}(\mathbf{A})$ in the next section. Thus the equality in (3) is understood in the sense of $(L^2(\Omega))^4$ and thus almost everywhere in Ω; and all the terms in $J(\tilde{\mathbf{U}})$ and $(G(\tilde{\mathbf{U}}), \bar{\mathbf{U}})$ are in $L^1(\Omega)$.

Now if we take instead of $\mathscr{V}$ the space $\mathscr{V}_1$ defined like $\mathscr{V}$ by replacing $L^2(\Omega)$ by $H^1(\Omega)$, i.e. we request more regularity on the groups of conservative variables, we can give an interpretation of (4). Indeed, let $\bar{\mathbf{U}}$ be in $(\mathscr{D}(\Omega))^4$; then we get, in the distribution sense,

$$\mathbf{A}^*(\mathbf{A}\tilde{\mathbf{U}}) = \mathbf{A}^*\mathbf{F}, \tag{5}$$

where the linear adjoint operator $\mathbf{A}^*$ is given by

$$\mathbf{A}^* = \begin{bmatrix}
-u\frac{\partial\cdot}{\partial x} - v\frac{\partial\cdot}{\partial y} & -[u^2 + (\gamma-1)e]\frac{\partial\cdot}{\partial x} - uv\frac{\partial\cdot}{\partial y} & -uv\frac{\partial\cdot}{\partial x} - [v^2(+\gamma-1)e]\frac{\partial\cdot}{\partial y} & -(\tfrac{1}{2}q^2u + \gamma eu)\frac{\partial\cdot}{\partial x} \\
 & & & -(\tfrac{1}{2}q^2v + \gamma ev)\frac{\partial\cdot}{\partial y} \\
-\rho\frac{\partial\cdot}{\partial x} & -2\rho u\frac{\partial\cdot}{\partial x} - \rho v\frac{\partial\cdot}{\partial y} & -\rho v\frac{\partial\cdot}{\partial x} & -(\tfrac{3}{2}\rho u^2 + \tfrac{1}{2}\rho v^2)\frac{\partial\cdot}{\partial x} \\
 & & & -\gamma\rho e\frac{\partial\cdot}{\partial x} - \rho uv\frac{\partial\cdot}{\partial y} \\
-\rho\frac{\partial\cdot}{\partial y} & -\rho u\frac{\partial\cdot}{\partial y} & -\rho u\frac{\partial\cdot}{\partial x} - 2\rho v\frac{\partial\cdot}{\partial y} & -\rho vu\frac{\partial\cdot}{\partial x} - \gamma\rho e\frac{\partial\cdot}{\partial y} \\
 & & & -(\tfrac{1}{2}\rho u^2 + \tfrac{3}{2}\rho v^2)\frac{\partial\cdot}{\partial y} \\
0 & -(\gamma-1)\rho\frac{\partial\cdot}{\partial x} & -(\gamma-1)\rho\frac{\partial\cdot}{\partial y} & -\gamma\rho u\frac{\partial\cdot}{\partial x} - \gamma\rho v\frac{\partial\cdot}{\partial y}
\end{bmatrix}$$

Then, with the additional regularity, this equality is meaningful in the sense of $(L^2(\Omega))^4$ and consequently almost everywhere in Ω. Thus we have transformed the first-order hyperbolic linear system (2) into a second-order linear system of parabolic type; for instance, if $\mathbf{A}$ reduces to its main diagonal, we find that the characteristic polynomial of $\mathbf{A}^*\mathbf{A}$ is

$$\det = \gamma^2\rho^6\varphi_y^8(-\tau u + v)^4(-2\tau u + v)^2(\tau u + 2v)^2$$

and thus $\mathbf{A}^*\mathbf{A}$ is a degenerated elliptic operator. In fact $\mathbf{A}$ and $\mathbf{A}^*$ have the same characteristic polynomial, and that of $\mathbf{A}^*\mathbf{A}$ is equal to the square of it. In the next section we show how we can set the boundary conditions to get a well posed problem equivalent to problem (3).

BOUNDARY CONDITIONS

For the Euler model one generally imposes different boundary conditions for subsonic flows and supersonic flows according to the number of characteristic curves entering in the associated unsteady problem. So, on one hand, the whole flow is given upstream and no condition is imposed downstream for supersonic flows and, on the other hand, one less condition is given upstream and one condition is imposed downstream for subsonic flows. For example, in two space dimensions the entropy and the flow direction are imposed in the entrance section and the pressure is specified in the exit section in subsonic flow. In three space dimensions this is not always possible, in particular for vortex flows where the vortex sheet must propagate downstream. For unsteady flows we can use non-reflecting boundary conditions as explained in Reference 6, but the situation seems to be less clear in the steady case. For the steady Euler equations we have chosen in our methodology to impose all the flow variables upstream and no variable downstream in supersonic as well as in subsonic flows. This is consistent with the fact that, on one hand, upstream influence is possible in subsonic flow via the centred discretization used and, on the other hand, the conservation equations are satisfied near the downstream boundary. Furthermore, the flow domain is unbounded and the obstacle has a finite length, so there is no explicit physical boundary condition to apply.

We show now how the least squares formulation associated with these boundary conditions is equivalent to solving the first-order system. We first define parts of the boundary as follows:

Γ_i, the entrance section where $\mathbf{q}_\infty \cdot \mathbf{n} < 0$

Γ_o, the exit section where $\mathbf{q}_\infty \cdot \mathbf{n} > 0$

Γ_w, the wing contour or surface where $\mathbf{q} \cdot \mathbf{n} = 0$ is imposed

Γ_s, the part of the exterior boundary where $\mathbf{q} \cdot \mathbf{n} = 0$ is imposed (for instance by symmetry).

We then set the conditions

$$\begin{cases} \tilde{\mathbf{q}} \cdot \mathbf{n} = 0 & \text{on } \Gamma_w \cup \Gamma_s, \\ \tilde{\mathbf{U}} \equiv 0 & \text{on } \Gamma_i \end{cases} \tag{6}$$

and define the space

$$\mathscr{D}(\mathbf{A}) = \{\tilde{\mathbf{U}} \in \tilde{\mathscr{V}} \text{ satisfying (6)}\}.$$

Now with $\tilde{\mathbf{U}} \in \mathscr{D}(\mathbf{A})$ and $\bar{\mathbf{U}} \in (H^1(\Omega))^4$ we get from (3)

$$\begin{aligned}
(\mathbf{A}\tilde{\mathbf{U}}, \bar{\mathbf{U}}) = (\tilde{\mathbf{U}}, \mathbf{A}^*\bar{\mathbf{U}}) &+ \int_{\partial\Omega} [\tilde{\rho}\bar{\rho}(\mathbf{q}\cdot\mathbf{n}) + \rho\bar{\rho}(\tilde{\mathbf{q}}\cdot\mathbf{n})]\,\mathrm{d}\sigma \\
&+ \int_{\partial\Omega} [\tilde{\rho}u\bar{u}(\mathbf{q}\cdot\mathbf{n}) + \tilde{\rho}v\bar{v}(\mathbf{q}\cdot\mathbf{n}) + (\gamma-1)\tilde{\rho}e(\bar{\mathbf{q}}\cdot\mathbf{n}) \\
&+ \rho\tilde{u}\bar{u}(\mathbf{q}\cdot\mathbf{n}) + \rho\tilde{v}\bar{v}(\mathbf{q}\cdot\mathbf{n}) + (\gamma-1)\rho\tilde{e}(\bar{\mathbf{q}}\cdot\mathbf{n}) \\
&+ \rho\tilde{u}\bar{u}(\tilde{\mathbf{q}}\cdot\mathbf{n}) + \rho v\bar{v}(\tilde{\mathbf{q}}\cdot\mathbf{n})]\,\mathrm{d}\sigma \\
&+ \int_{\partial\Omega} [\tilde{\rho}(\gamma e + \tfrac{1}{2}q^2)\bar{e}(\mathbf{q}\cdot\mathbf{n}) + \gamma\rho e\bar{e}(\tilde{\mathbf{q}}\cdot\mathbf{n}) + \gamma\rho\tilde{e}\bar{e}(\mathbf{q}\cdot\mathbf{n}) \\
&+ \tfrac{1}{2}\rho u^2\bar{e}(\tilde{\mathbf{q}}\cdot\mathbf{n}) + \tfrac{1}{2}\rho v^2\bar{e}(\tilde{\mathbf{q}}\cdot\mathbf{n}) \\
&+ \rho u\tilde{u}\bar{e}(\mathbf{q}\cdot\mathbf{n}) + \rho v\tilde{v}\bar{e}(\mathbf{q}\cdot\mathbf{n})]\,\mathrm{d}\sigma.
\end{aligned}$$

Thus with $\mathbf{q}\cdot\mathbf{n}=0$ on $\Gamma_w \cup \Gamma_s$, in addition to (6) we get the adjoint boundary conditions

$$\begin{cases} \bar{\mathbf{q}}\cdot\mathbf{n}=0 & \text{on } \Gamma_w \cup \Gamma_s, \\ \bar{\mathbf{U}}=0 & \text{on } \Gamma_o \end{cases} \tag{7}$$

and define the space

$$\mathscr{D}(\mathbf{A}^*)=\{\bar{\mathbf{U}}\in(H^1(\Omega))^4;\quad \bar{\mathbf{U}} \text{ satisfies (7)}\}.$$

Then from equation (5) with $\bar{\mathbf{U}}\in\mathscr{D}(\mathbf{A})$ we get

$$(\mathbf{A}^*(\mathbf{A}\tilde{\mathbf{U}}-\mathbf{F}), \bar{\mathbf{U}})=(G(\tilde{\mathbf{U}}), \bar{\mathbf{U}})$$

if $\mathbf{A}\tilde{\mathbf{U}}-\mathbf{F}\in\mathscr{D}(\mathbf{A}^*)$ (which needs the additional regularity $\mathbf{U}\in\mathscr{V}_1$). Finally, (4) is equivalent to solving

$$\begin{cases} \mathbf{A}^*(\mathbf{A}\tilde{\mathbf{U}})=\mathbf{A}^*\mathbf{F} & \text{in } \Omega, \\ \tilde{\mathbf{U}}\in\mathscr{D}(\mathbf{A}), \\ \mathbf{A}\tilde{\mathbf{U}}-\mathbf{F}\in\mathscr{D}(\mathbf{A}^*) \end{cases} \tag{8}$$

and this problem is equivalent to the initial linear problem (3) under the condition that $\mathbf{A}^*$ is a one-to-one operator and admits a unique solution under the condition that $\mathbf{A}$ is a one-to-one operator.

We see that on Γ_o, where no condition is given, the least squares formulation forces the equations to be satisfied and yields a well posed linear problem, the solution of which can be computed without artifacts (artificial viscosity or Kutta condition).

Remark. Here the condition $\mathbf{q}\cdot\mathbf{n}=0$ reduces to $v=0$ or $w=0$, but for more complex geometries it is not so easy to impose such a non-linear condition; once again the least squares formulation is helpful because we can add a boundary term in the functional $J(\tilde{\mathbf{U}})$ as follows:[4]

$$\frac{1}{2}\int_{\Gamma_w}[(\mathbf{q}-\bar{\mathbf{q}})\cdot\mathbf{n}]^2 d\sigma,$$

and thus the next iterate $\mathbf{U}_{m+1}$ of the Newton method satisfies the tangency condition on the wing.

APPROXIMATION

In order that this paper be relatively self-contained, we give a short description of the finite element approximation. Let W be a Hilbert space on which is set a variational problem

$$\begin{cases} \text{find } u\in W \text{ such that} \\ a(u, v)=l(v) \quad \forall v\in W, \end{cases} \tag{9}$$

where a is a W-elliptic continuous bilinear form and l is a continuous linear form on W; the purpose of the finite element method is to construct a finite-dimensional space W_h approximating W such that either $W_h\subset W$ or $W_h\not\subset W$. We restrict our study to the conforming case ($W_h\subset W$) for which the approximated variational problem reads

$$\begin{cases} \text{find } u_h\in W_h \text{ such that} \\ a(u_h, v_h)=l(v_h) \quad \forall v_h\in W_h, \end{cases} \tag{10}$$

where a and l have the same definition. If we define W_h and construct its basis, the problem (10) is completely determined and yields a linear system we can solve by any inversion method.

Now we see how to construct a conforming approximation of the space $H^1(\Omega)$ by means of a $\mathbb{Q}^1$ finite element in a regular domain of $\mathbb{R}^3$. Let K be a regular hexaedron in $\mathbb{R}^3$ with vertices (a_k),

$k=1, \ldots, 8$; we define the set of degrees of freedom

$$\Sigma_K=\{l_k: p\in P_K \to p(a_k)\in \mathbb{R};\ k=1, \ldots, 8\}$$

and the space of polynomials

$$P_K=\text{span}\{1, x, y, z, xy, xz, yz, xyz\};$$

then $\mathbb{Q}1$ denotes the finite element (K, Σ_K, P_K). In a regular domain as shown in Figure 1 we can easily construct a mesh made of regular hexahedra and define the space

$$W_h=\{w_h\in C^0(\bar{\Omega}) \text{ such that } w_h/K\in \mathbb{Q}1 \text{ for each } K\},$$

the dimension of which is equal to the number of vertices (a_i), $i=1, \ldots, I$, of the mesh and the basis of which is given by $\phi_i(a_j)=\delta_{ij}$, $1\leqslant i, j\leqslant I$, where δ_{ij} is the Kronecker symbol. Moreover, this space is included in $H^1(\Omega)$ and then (10) is a conforming approximation of (9).

Here we introduce the spaces

$\mathscr{V}_h=\{\mathbf{U}_h\in(L^\infty(\Omega))^4,\ \mathbf{U}_h>\mathbf{0}$ such that every group of approximate variables $(\rho_h u_h, \ldots)$ belongs to $W_h\}$,

$\tilde{\mathscr{V}}_h=\{\tilde{\mathbf{U}}_h\in(L^2(\Omega))^4$ such that every group of mixed approximate variables $(\tilde{\rho}_h u_h, \ldots)$ belongs to $W_h\}$,

$$\mathscr{D}_h(\mathbf{A})=\{\tilde{\mathbf{U}}_h\in\tilde{\mathscr{V}}_h \text{ satisfying (6)}\}$$

and the approximate problem of (4) reads

$$\begin{cases}\text{find } \tilde{\mathbf{U}}_h\in\mathscr{D}_h(\mathbf{A}) \text{ such that}\\ (G(\tilde{\mathbf{U}}_h), \bar{\mathbf{U}}_h)=0 \quad \forall\bar{\mathbf{U}}_h\in\mathscr{D}_h(\mathbf{A}).\end{cases} \tag{11}$$

This problem is a conforming approximation of (4) with a centred scheme where not the unknowns separately but the groups of variables are approximated by the finite element method; for instance, we write

$$\tilde{\rho}_h u_h=\sum_{i=1}^{I}(\tilde{\rho}u)_i\phi_i,$$

where $(\tilde{\rho}u)_i=\tilde{\rho}_i u_i$ is the value of the group $\tilde{\rho}_h u_h$ at the vertex a_i of the mesh. This is the main point of the approximation; indeed, requiring $\tilde{\rho}_h$ and u_h separately to belong to W_h would impose too much regularity on the variables and would not allow the shocks and the contact discontinuities. Furthermore, this is the more natural way to realize a conforming approximation of the space $\mathscr{D}(\mathbf{A})$ and we have the following result:

$$\text{problem (11) admits a unique solution } \tilde{\mathbf{U}}_h\in\mathscr{D}_h(\mathbf{A}).$$

Proof. Obviously the result will be achieved if we prove that $|\mathbf{A}\tilde{\mathbf{U}}_h|_{(L^2(\Omega))^4}$ is a norm over the space $\mathscr{D}_h(\mathbf{A})$. In order to simplify the proof, we consider a mesh in a 2D tube and $K=[0, 1]\times[0, 1]$; we denote by $\tilde{\rho}_h u_h/K$ the restriction of $\tilde{\rho}_h u_h$ to K. As a first step we show that if $\mathbf{A}\tilde{\mathbf{U}}_h$ vanishes on K, then $\tilde{\mathbf{U}}_h/K\equiv\mathbf{0}$. A polynomial of $\mathbb{Q}1$ is written in its general form $a+bx+cy+dxy$, but with the boundary conditions upstream it reduces to $bx+dxy$; moreover, as v_h and $\tilde{v}_h$ vanish at point $(1, 0)$, we have

$$\tilde{\rho}_h u_h/K=p_1=b_1x+d_1xy, \qquad \tilde{\rho}_h v_h/K=p_2=d_2xy,$$
$$\rho_h\tilde{u}_h/K=p_3=b_3x+d_3xy, \qquad \rho_h\tilde{v}_h/K=p_4=d_4xy.$$

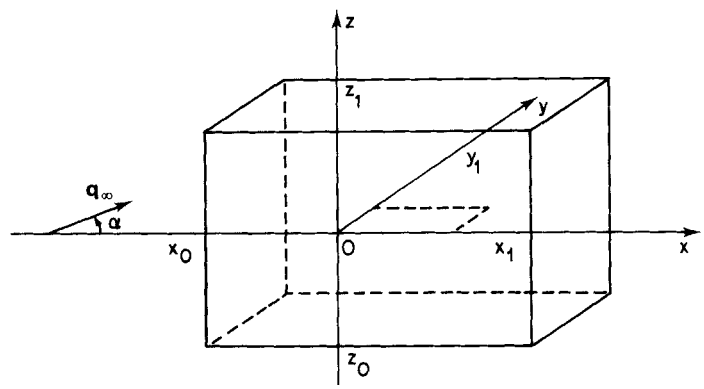

Figure 1. Domain

But from the first equation we have

$$\frac{\partial p_1}{\partial x}+\frac{\partial p_2}{\partial y}+\frac{\partial p_3}{\partial x}+\frac{\partial p_4}{\partial y}=0 \Leftrightarrow b_1+b_3+(d_2+d_4)x+(d_1+d_3)y=0;$$

then we get $p_1+p_3=0$ and $p_2+p_4=0$. But also we have

$$(\gamma-1)\tilde{\rho}_h e_h/K=p_5=b_5x+d_5xy, \qquad \rho_h u_h\tilde{u}_h/K=p_6=b_6x+d_6xy,$$
$$(\gamma-1)\rho_h\tilde{e}_h/K=p_7=b_7x+d_7xy, \qquad \rho_h\tilde{u}_h v_h/K=p_8=d_8xy,$$

and the second equation

$$\left(\frac{\partial\tilde{\rho}_h u_h^2}{\partial x}+\frac{\partial\tilde{\rho}_h u_h v_h}{\partial y}+\frac{\partial(\gamma-1)\tilde{\rho}_h e_h}{\partial x}+\frac{\partial 2\rho_h u_h\tilde{u}_h}{\partial x}+\frac{\partial\rho_h\tilde{u}_h v_h}{\partial y}+\frac{\partial\rho_h u_h\tilde{v}_h}{\partial y}+\frac{\partial(\gamma-1)\rho_h\tilde{e}_h}{\partial x}\right)\Big/K$$
$$=u_h\left(\frac{\partial p_1}{\partial x}+\frac{\partial p_2}{\partial y}+\frac{\partial p_3}{\partial x}+\frac{\partial p_4}{\partial y}\right)+(p_1+p_3)\frac{\partial u_h}{\partial x}+(p_2+p_4)\frac{\partial u_h}{\partial y}+\frac{\partial p_5}{\partial x}+\frac{\partial p_6}{\partial x}+\frac{\partial p_7}{\partial x}+\frac{\partial p_8}{\partial y}$$
$$=\frac{\partial p_5}{\partial x}+\frac{\partial p_6}{\partial x}+\frac{\partial p_7}{\partial x}+\frac{\partial p_8}{\partial y}=0$$
$$\Leftrightarrow b_5+b_6+b_7+d_8x+(d_5+d_6+d_7)y=0;$$

then $d_8=0$ and $\rho_h\tilde{u}_h v_h/K\equiv 0$ on K.

Proceeding in the same way with the third equation, we get $\rho_h u_h\tilde{v}_h/K\equiv 0$ on K and, as $\mathbf{q}_h$ cannot vanish on an element, we have either $\tilde{u}_h/K\equiv 0$ or $\tilde{v}_h/K\equiv 0$ and consequently $p_5+p_7=0$ (indeed $\tilde{u}_h/K\equiv 0$ implies $p_6=0$); thus we get $\tilde{u}_h/K\equiv 0$ from the equalities $p_1+p_3=p_2+p_4=p_5+p_7=0$. Now marching element by element on the first row from left to right, we get that $\tilde{u}_h$ vanishes on this first row. On the first element of the second row a polynomial of $\mathbb{Q}1$ reduces now to dxy and we can apply the same method to show that $\tilde{\mathbf{U}}_h$ vanishes on this element, then on the second row and finally everywhere on Ω; so $|\mathbf{A}\tilde{\mathbf{U}}_h|_{(L^2(\Omega))^4}$ is a norm over $\mathscr{D}_h(\mathbf{A})$.

Now the unique solution of problem (11) will be obtained by solving a linear system which, unfortunately, is not so easy to invert as we shall see in the next section.

STUDY AND INVERSION OF THE LINEAR SYSTEM

Let (11) be written in its matrix form:

$$\begin{cases} \text{find the vector } \mathbf{X} \text{ such that} \\ \mathbf{SX}=\mathbf{Y}. \end{cases} \tag{12}$$

We first look at the properties of the matrix **S**. From the least squares minimization and the proof above we know that **S** is a symmetric positive definite matrix. But if **A** is a one-to-one operator on $\mathscr{D}_h(\mathbf{A})$, it is not true in general on $\mathscr{D}(\mathbf{A})$; then **A** can have a kernel and a zero in its spectrum, so we can expect the matrix **S** to have small eigenvalues. Indeed, if the kernel is not included in $\mathscr{D}_h(\mathbf{A})$, its eigenvectors can be approached by the conforming method and thus the smallest eigenvalue of **S** should become smaller and smaller as the mesh size h goes to zero. We used the algorithm developed in Reference 7 based on a Lanczos tridiagonalization without reorthogonalization to compute the eigenvalues of **S** and found that the smallest eigenvalue decreases and the conditioning increases when h becomes smaller. This is illustrated in Table I at the first step of the Newton method with $\mathbf{U}_0$ uniformly defined equal to the values of the incoming flow for Mach number $M=0{\cdot}7$ and an angle of attack $\alpha=15°$ (the results are about the same for $M=2$, $\alpha=10°$ and if $\mathbf{U}_0$ is replaced by an iterated solution); so we have to find the right method to solve (12).

For our regular domain (see figure 1) **S** is a block-structured symmetric matrix where each block represents the contribution of a vertical plane parallel to $(0, y, z)$ and (12) can be rewritten as a block tridiagonal system:

$$\begin{pmatrix} \mathbf{E}_1\mathbf{F}_1 & & & \\ \mathbf{F}_1^{\mathrm{T}}\mathbf{E}_2\mathbf{F}_2 & & & \\ & & & \mathbf{F}_{N-1} \\ & & \mathbf{F}_{N-1}^{\mathrm{T}} & \mathbf{E}_N \end{pmatrix} \begin{pmatrix} \mathbf{X}_1 \\ \mathbf{X}_2 \\ \\ \mathbf{X}_N \end{pmatrix} = \begin{pmatrix} \mathbf{Y}_1 \\ \mathbf{Y}_2 \\ \\ \mathbf{Y}_N \end{pmatrix}. \tag{13}$$

Until now, the most efficient way we have found to solve this system is to use a block successive over-relaxation (BSOR) algorithm where the diagonal blocks $\mathbf{E}_n$ are inverted by the incomplete Cholesky conjugate gradient (ICCG) method. However, the $\mathbf{E}_n$ blocks are so ill conditioned that we need an additional shifting term to stabilize the whole process; thus the shifted block successive over-relaxation (SBSOR) algorithm reads

$$\begin{cases} (\mathbf{E}_n+\beta\mathbf{D}_n)\bar{X}_n^{j+1}=\mathbf{Y}_n-\mathbf{F}_{n-1}^{\mathrm{T}}X_{n-1}^{j+1}-\mathbf{F}_nX_{n+1}^{j}+\beta\mathbf{D}_nX_n^{j}, \\ X_n^{j+1}=\omega\bar{X}_n^{j+1}+(1-\omega)X_n^{j}, \end{cases} \tag{14}$$

where β, $0<\beta<1$, is the shift parameter, ω, $1\leqslant\omega<2$, is the over-relaxation parameter and $\mathbf{D}_n$ is the main diagonal of $\mathbf{E}_n$. Of course if $\beta=0$ we have the usual BSOR algorithm, and if we add the whole block $\mathbf{E}_n$ instead of $\mathbf{D}_n$ in (14) we have also the usual BSOR algorithm with a new relaxation parameter $\delta=\omega/(1+\beta)$. What we want to do is to correct the conditioning of the blocks we have to

Table I

h	Number of unknowns	Smallest eigenvalue	Largest eigenvalue	Conditioning
0·0475	1470	$0{\cdot}4248\times10^{-4}$	8·63	$0{\cdot}20316\times10^{6}$
0·0211	7700	$0{\cdot}8401\times10^{-5}$	6·86	$0{\cdot}81694\times10^{6}$
0·01	53200	$0{\cdot}1294\times10^{-5}$	8·24	$0{\cdot}63671\times10^{7}$

invert; this is achieved by the consistent algorithm (14) for which we do not know how to prove the convergence compared with that of the BSOR algorithm. Nevertheless, we show numerically on the Laplace problem in the square $(0, 1) \times (0, 1)$ that the algorithm (14) converges as illustrated in Table II and in Figure 2 where the convergence history for several values of β is plotted.

Thus we have to take β as small as possible; in practice we set $\beta = 0{\cdot}1$ and $\omega = 1{\cdot}5$ for our problem. As solving (14) is embedded into the iterations of the Newton linearization , it is not

Table II

Mesh size	ω	β	Error	Number of iterations
		0	$0{\cdot}31 \times 10^{-3}$	13
0·1	1·41	0·1	$0{\cdot}36 \times 10^{-3}$	25
		0·5	$0{\cdot}46 \times 10^{-3}$	65
		1	$0{\cdot}48 \times 10^{-3}$	114
		0	$0{\cdot}15 \times 10^{-3}$	30
0·05	1·64	0·1	$0{\cdot}17 \times 10^{-3}$	78
		0·5	$0{\cdot}20 \times 10^{-3}$	243
		1	$0{\cdot}20 \times 10^{-3}$	449
		0	$0{\cdot}95 \times 10^{-4}$	83
0·02	1·84	0·1	$0{\cdot}98 \times 10^{-4}$	388
		0·5	$0{\cdot}99 \times 10^{-4}$	1486
		1	—	—

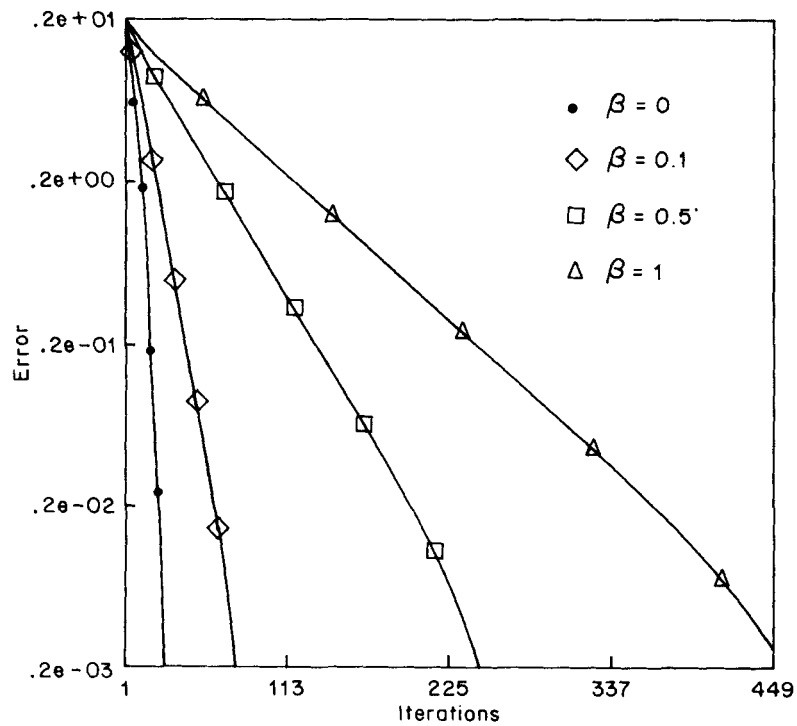

Figure 2. Convergence history of SBSOR algorithm with respect to BSOR algorithm for mesh size $h = 0{\cdot}05$

necessary to compute **X** very accurately, so a few iterations (5–10) of SBSOR is enough. Moreover, setting the parameter β to a good value improves the efficiency of the ICCG method and yields a very good solution rapidly; otherwise (β too small) the ICCG method cannot converge and the approximated $\mathbf{X}_n$ are spoiled.

VECTORIZATION OF PROGRAMS

The programs run on a CRAY-2 and the main part of the CPU time is devoted to the construction and inversion of system (13), so we shall speak only of the vectorization of these two actions. With the approximation of groups of variables described above, the assembling of the matrix is reduced to a product of an initial matrix and a vector; for instance, the term

$$\int_\Omega \frac{\partial \bar{\rho}_h u_h}{\partial x} \frac{\partial \bar{\rho}_h u_h}{\partial x} \, dx dy$$

yields the matrix coefficients

$$u_i u_j \int_\Omega \frac{\partial \phi_i}{\partial x} \frac{\partial \phi_j}{\partial x} \, dx dy$$

for $1 \leqslant i \leqslant I$ and some j corresponding to the basis functions ϕ_j whose support intersects with the support of ϕ_i. For a regular domain these indices j are always the same with respect to i and **S** is a multidiagonal matrix which can be easily computed knowing the initial matrices **DXX**, **DXY**, etc. representing the terms

$$\int_\Omega \frac{\partial \phi_i}{\partial x} \frac{\partial \phi_j}{\partial x} \, dx dy, \qquad \int_\Omega \frac{\partial \phi_i}{\partial x} \frac{\partial \phi_j}{\partial y} \, dx dy, \qquad \text{etc.;}$$

so we use the huge memory of CRAY-2 to store these initial matrices and then the assembling of the matrix at each iteration of the Newton linearization is written as follows.

For *i*diag = 1 to the number of diagonals of a block do:

nj = the position of the diagonal *i*diag with respect to the main diagonal.
For *i*dlib = 1 to *I* do:
*j*dlib = *i*dlib + *nj*,
$\mathbf{E}_n(i\text{dlib}, i\text{diag}) = u(i\text{dlib}) \times (\mathbf{DXX}(i\text{dlib}, i\text{diag}) \times u(j\text{dlib})$
$+ \mathbf{DXY}(i\text{dlib}, i\text{diag}) \times v(j\text{dlib})) + \ldots,$
End.
End

Thus the inner loop of large size is vectorized. For an irregular domain we can do the same with an outer loop to the number of non-zero terms and the use of the function GATHER to avoid the indirect addressing of *j*dlib in the sequence above. So in both cases the assembling is highly vectorizable.

For the inversion of the blocks in (14) the vectorization is *a priori* more difficult because the Cholesky factorization is a typical operation which involves dependency, but we benefit from the 5×5 block structure related to the five unknowns in dimension three. Indeed, each block $\mathbf{E}_n$ or $\mathbf{F}_n$ is divided into 25 equal sub-blocks and the Cholesky factorization is always vectorizable except when it occurs on the same sub-block; so about 80% of the factorization is vectorized and we reach a very good performance in terms of Mflops on the whole program.

NUMERICAL RESULTS

In this section we present results illustrating the influence of mesh size, angle of attack and Mach number at infinity on the solution. In Figure 3 we show the two meshes in a cross-plate section; the coarse one is only $14 \times 9 \times 9$ and the second one is $28 \times 18 \times 18$ cells around the same flat plate without thickness. The numbers of variables are respectively 8250 and 55100.

The solution for $M_\infty = 0{\cdot}7$ and $\alpha = 15°$ is shown in Figure 4–7 in cross-flow sections and on the upper side of the plate; we see that the vortex structure rolls up at the tip of the plate with a typical

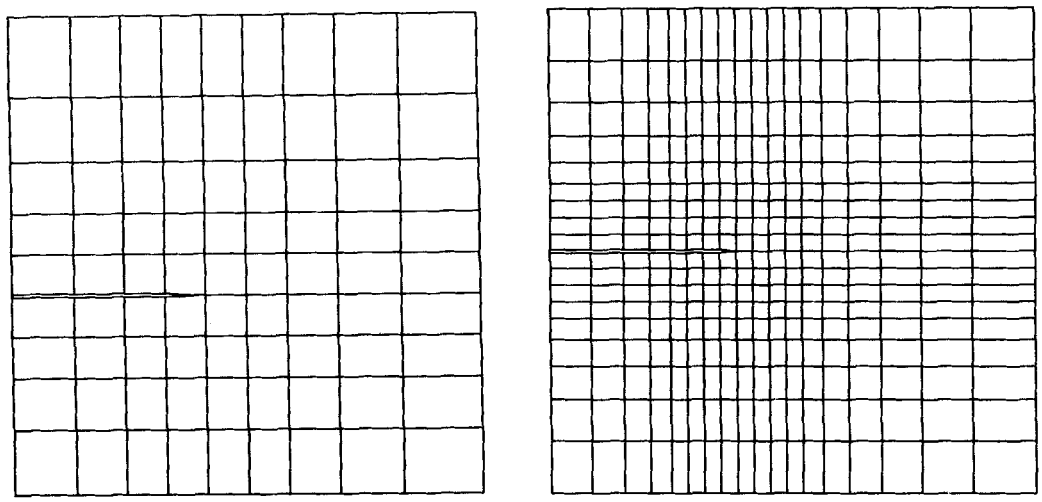

Figure 3. Meshes in a cross-plate section

(a) $14 \times 9 \times 9$ cells

(b) $28 \times 28 \times 18$ cells

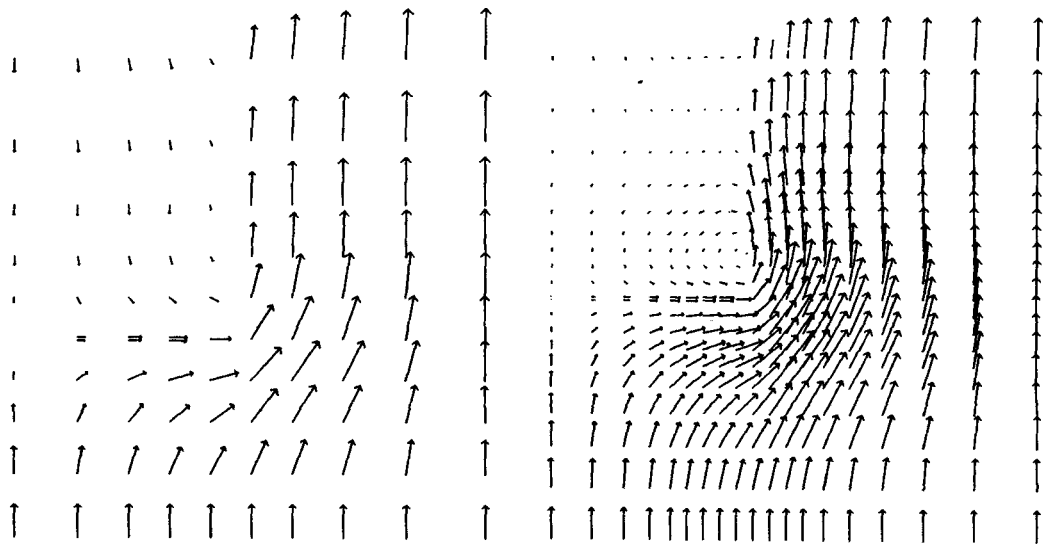

Figure 4. Comparison of the cross-flow velocities at 60% of the plate for the two meshes ($M_\infty = 0{\cdot}7$, $\alpha = 15°$)

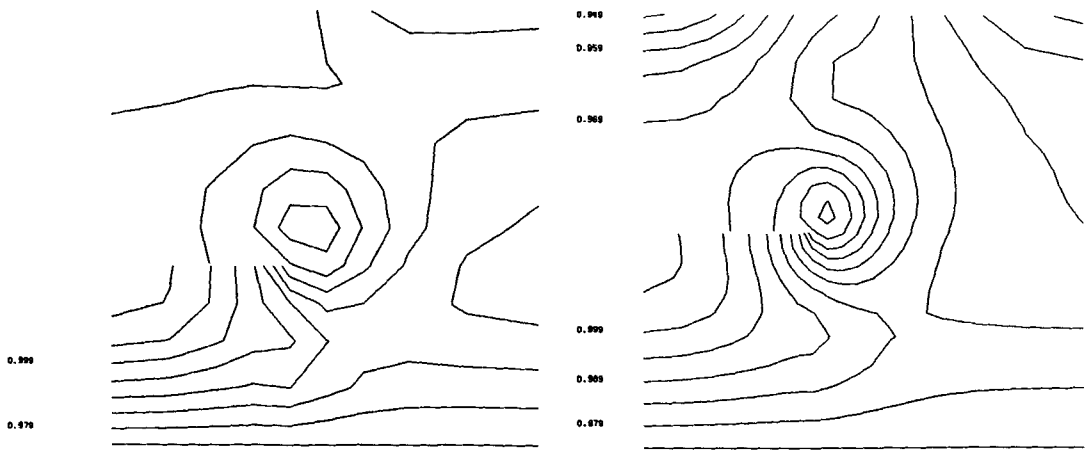

Figure 5. Comparison of isobars in a cross-plane at 60% of the plate for the two meshes ($M_\infty = 0{\cdot}7$, $\alpha = 15°$)

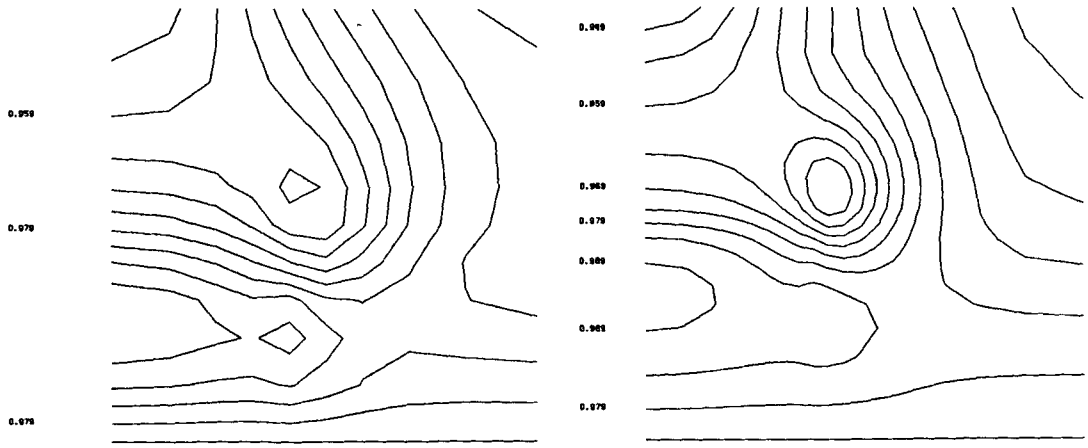

Figure 6. Comparison of isobars in a cross-plane at the trailing edge for the two meshes ($M_\infty = 0{\cdot}7$, $\alpha = 15°$)

aspect of the isobar lines as shown in Figure 7. Of course the solution is better represented by the finer mesh, although the vortex centre is located at the same place in both cases. Thus our method is able to capture the main behaviour of the flow even with a coarse mesh.

We now see the influence of the angle of attack by comparing Figures 4–7 for the finer mesh with Figures 8–10 where the solution for a higher angle of attack, $\alpha = 30°$, is plotted. One can see clearly that the size of the vortex structure and the amplitude of the pressure jump on both sides of the plate are linked directly to the angle of attack.

Finally, we have done computations for supersonic flows with $M_\infty = 2$ and $\alpha = 10°$; we notice that the vortical phenomenon is again well captured, as shown in Figures 11 and 12. In this case the vortex is closer to the plate and perturbations in pressure and flow direction are visible near the upper boundary which is located not very far away.

It is interesting to note that solving the steady energy equation does not imply that the total enthalpy is constant everywhere, but the results indicate that the error on total enthalpy does not exceed 3% and that the maximum is reached in the vortex core.

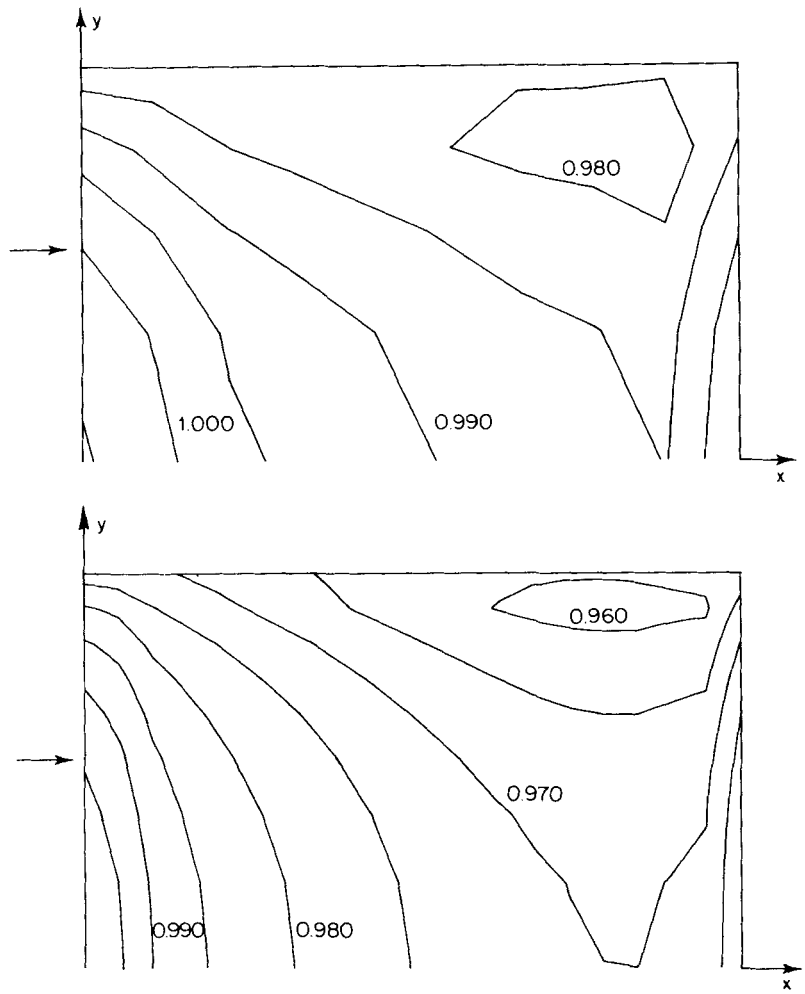

Figure 7. Comparison of isobars on the upper plate for the two meshes ($M_\infty = 0{\cdot}7$, $\alpha = 15°$); pressure of the incoming flow, $p_\infty = 0{\cdot}975$

CONCLUSIONS

The method presented in this paper is able to capture vortical effects in subsonic flows as well as in supersonic flows. We have shown from a mathematical point of view that the least squares formulation is equivalent to the original first-order Euler system. We have imposed all the flow variables at the entrance boundary and no condition at the exit boundary in both subsonic and supersonic flows, and we were able to compute solutions for various Mach numbers and angles of attack. However, in supersonic flow, when the incidence is larger than the characteristic cone half-angle, the boundary conditions coincide with the usual ones.

All the computations have been performed without the use of artificial viscosity. The centred finite element scheme of second-order accuracy employed in the solution procedure is stable owing to its inherent dissipative properties, which may explain why there is no need for a Kutta condition at the plate edges to provoke the shedding of vorticity.

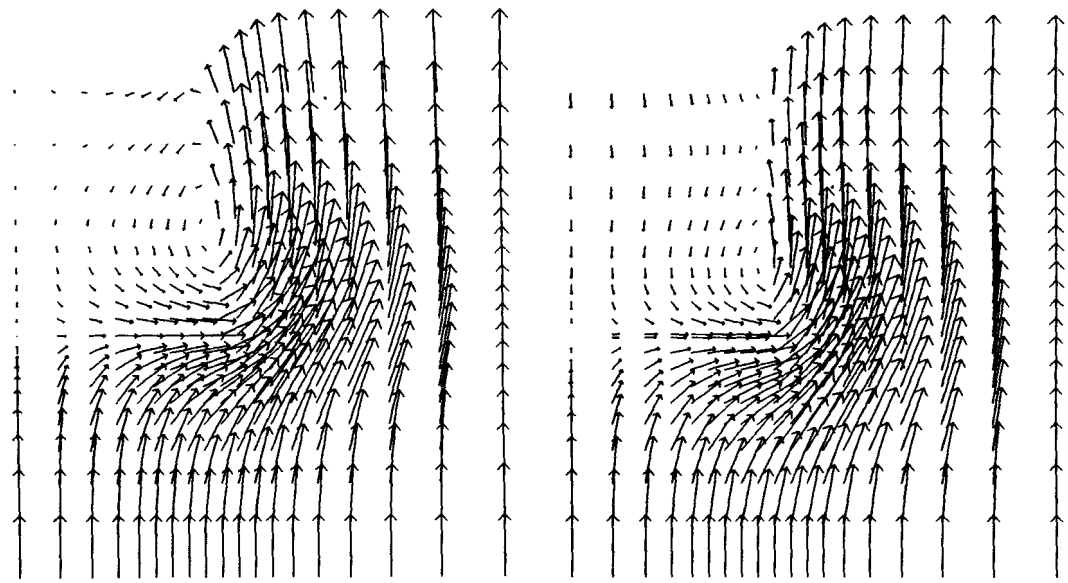

Figure 8. Cross-flow velocities at 60% of the plate and at the trailing edge for $M_\infty = 0{\cdot}7$ and $\alpha = 30°$

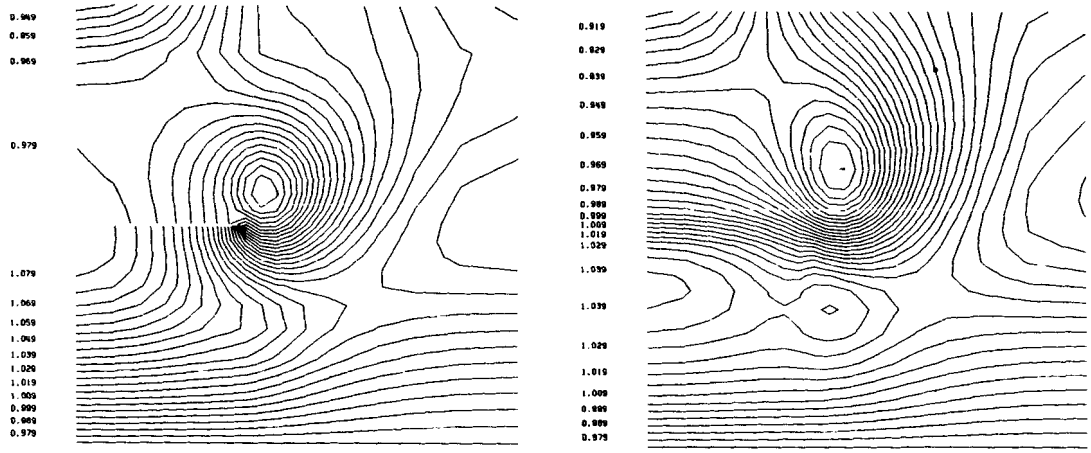

Figure 9. Isobars in cross-planes at 60% of the plate and at the trailing edge for $M_\infty = 0{\cdot}7$ and $\alpha = 30°$

Moreover, we still get a vortex flow in a hypersonic case with $M_\infty = 5$ and $\alpha = 10°$ as illustrated in Figure 13; this shows the robustness of the method.

ACKNOWLEDGEMENTS

This work was performed with financial support from DRET and under grants from C²VR, Ecole Polytechnique, France.

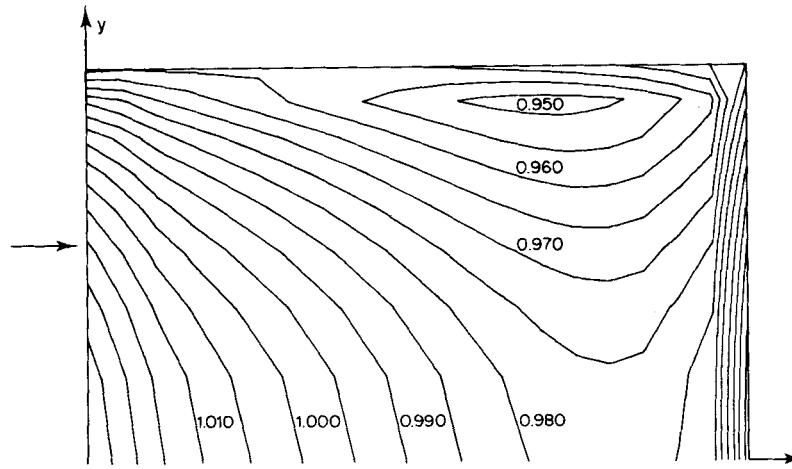

Figure 10. Isobars on the upper plate for $M_\infty = 0{\cdot}7$ and $\alpha = 30°$

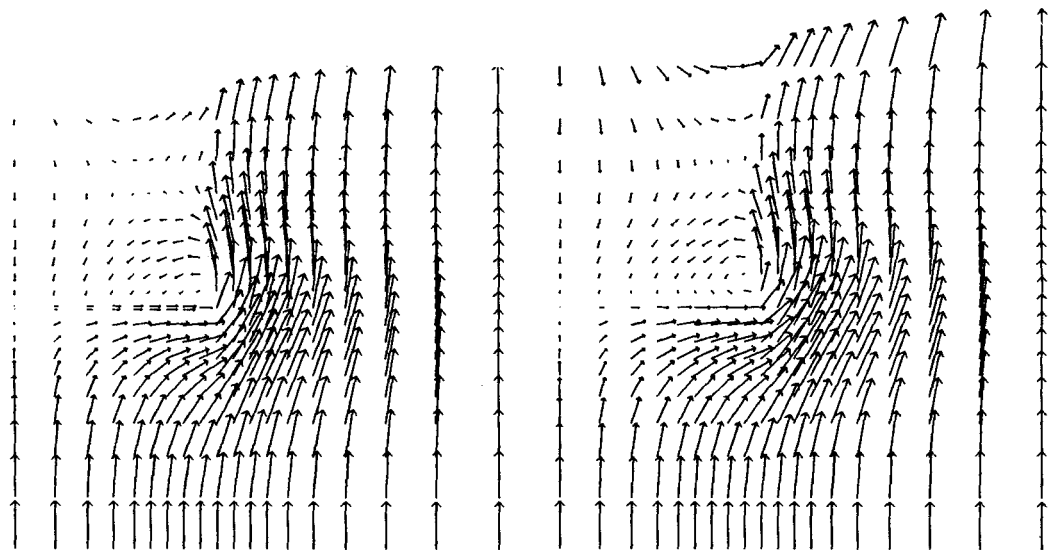

Figure 11. Cross-flow velocities at 60% of the plate and at the trailing edge for $M_\infty = 2$ and $\alpha = 10°$

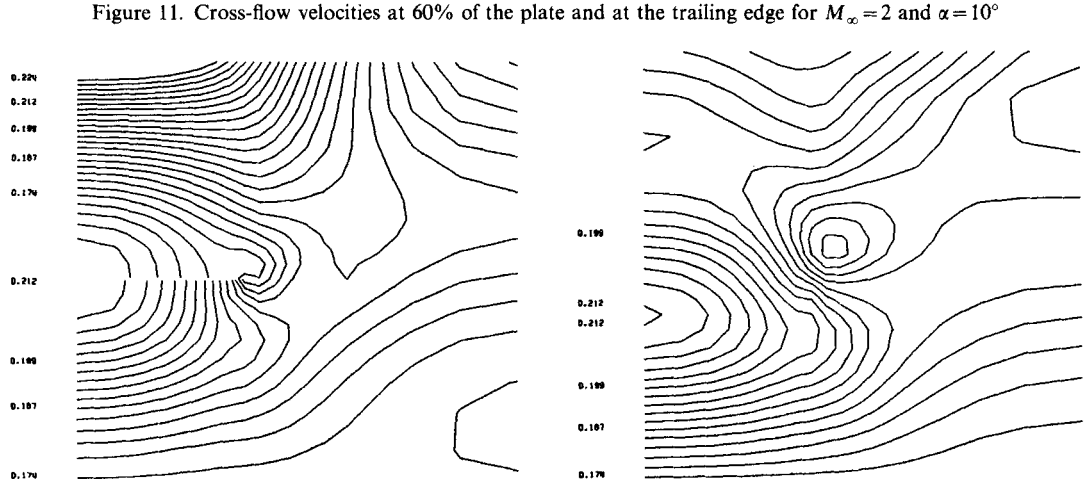

Figure 12. Isobars in cross-planes at 60% of the plate and at the trailing edge for $M_\infty = 2$ and $\alpha = 10°$

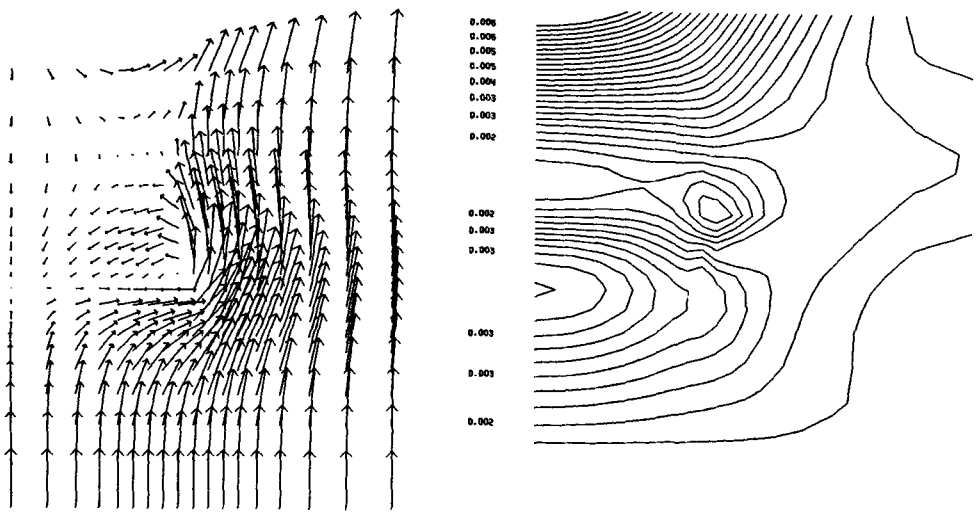

Figure 13. Hypersonic solution at the trailing edge ($M_\infty = 5$, $\alpha = 10°$)

REFERENCES

1. A. Rizzi and Ch. J. Purcell, 'On the computation of transonic leading-edge vortices using the Euler equations', *J. Fluid Mech.*, **181**, 163–195 (1987).
2. O. A. Kandil, A. H. Chuang and J. M. Shifflette, 'Finite-volume Euler and Navier–Stokes solvers for three-dimensional and conical vortex flows over delta wings', *AIAA Paper 87-0041*, 1987.
3. R. W. Newsome, 'Euler and Navier–Stokes solutions for flow over a conical delta wing', *AIAA J.* **24**, 552–561 (1986).
4. Ch. H. Bruneau, J. J. Chattot, J. Laminie and R. Temam, 'Numerical solutions of the Euler equations with separation by a finite element method', *9th ICNMFD*, Saclay; *Lecture Notes in Physics 218*, 1984, pp. 121–126.
5. Ch. H. Bruneau, J. J. Chattot, J. Laminie and R. Temam, 'Computation of vortex flows past a flat plate at high angle of attack', *10th ICNMFD*, Beijing; *Lecture Notes in Physics 264*, 1986, pp. 134–140.
6. G. W. Hedstrom, 'Non reflecting boundary conditions for nonlinear hyperbolic systems', *J. Comput. Phys.*, **30**, 222–237 (1979).
7. J. Cullum and R. A. Willoughby, 'Computing eigenvalues of very large symmetric matrices—an implementation of a Lanczos algorithm with no reorthogonalization', *J. Comput. Phys.*, **44**, 329–358 (1981).